DYNATECH CORPORATION

THE USE OF FLOW-THROUGH ELECTRODES IN A HIGH CURRENT DENSITY HYDROGEN-OXYGEN FUEL CELL STACK

FINAL REPORT

December 5, 1966 to April 5, 1967

Prepared by:

Dr. Adrian R. Reti
Dr. Shafik Sadek

Prepared for:

Code RNW
National Aeronautics & Space Administration
Washington, D.C. 20546

Contract NAS 7-530

June 12, 1967

Progress through Research

THE USE OF FLOW-THROUGH ELECTRODES IN A HIGH CURRENT DENSITY HYDROGEN-OXYGEN FUEL CELL STACK

FINAL REPORT

December 5, 1966 to April 5, 1967

Prepared by:

Dr. Adrian R. Reti
Dr. Shafik Sadek

Prepared for:

Code RNW
National Aeronautics & Space Administration
Washington, D. C. 20546

Contract NAS 7-530

June 12, 1967

Dynatech Report No. 719
Dynatech Project No. NAS-20

DYNATECH CORPORATION
17 Tudor Street
Cambridge, Massachusetts 02139
617-868-8050

TABLE OF CONTENTS

LIST OF FIGURES

Section 1

SUMMARY

The present project consisted of an analytical study of the performance of a flow-through-electrode, hydrogen-oxygen fuel cell stack. The purpose of this study was to compare the potential system weight with those of other power sources, such as silver-zinc batteries and other fuel cell systems. It can thus be established whether or not there is a mission duration for which use of flow-through electrodes is advantageous. It was found that an efficiently packaged system, operating at electrolyte saturator pressures of 10 to 50 atm, should deliver 300 to 500 watt-hours per pound of total system weight for a 24-hour mission, and 100 to 150 watt-hours per pound for a 5-hour mission. The system appears to have no advantages for longer missions.

Overall system performance was calculated with confidence, since all kinetic and mass transfer input data have an experimental basis. The performance of such high current-density flow-through electrodes, however, should be confirmed experimentally, since the calculations are based on simplified, idealized structures. The performance of the saturators needs experimental confirmation as well, not as much in terms of achievable mass-transfer rates as to ascertain whether any flow or side leakage problems are encountered with such controlled wetting structures.

The total system weight was found to be relatively insensitive to electrode current density in the 0.15 to 0.40 ampere/cm^2 range. The optimum saturator pressure was found to be between 20 and 50 atm for all cases.

If further development of such a system proves to be desirable, it is recommended that the performance of the saturator structures described in this report be confirmed experimentally. An experimental check of the predicted electrode performances would be desirable as well, since flow-through oxygen and hydrogen electrodes have not been operated yet at the high reactant concentrations at which optimum system weights are achieved.

Section 2

INTRODUCTION

The present project was performed in response to NASA's requirement for new concepts in fuel-cell reactor design, with the potential of achieving higher specific power outputs and of resulting in simpler and more rugged and reliable systems.

The concept studied by Dynatech incorporates as its basic feature the use of "flooded" or "flow-through" electrodes. Such "flow-through" electrodes are not new to the fuel cell field. The author successfully operated such devices as early as 1960 (Refs. 1, 2), and more exhaustive although idealized mathematical analyses of such electrodes were later performed by Tobias and coworkers at the University of California. The main emphasis on such devices was on their use as a research tool or their application in conjunction with soluble fuels.

The potential practical application of this concept to H_2-O_2 fuel cells, however, has not been either fully understood or brought into practice.

In all current gas-fueled fuel cells the electrode structure serves a multiplicity of functions such as:

1. Carrying the electrical current to the current collectors.
2. Providing the catalytic surface for chemisorption and the electrochemical reaction to take place.
3. Separating the liquid from the gaseous phase while providing the interfacial area for the reactant solution-diffusion and the reaction product diffusion-removal processes to take place.

Considerable insight has been gained into the way in which all these processes take place. The electrochemical kinetics have been successfully isolated from the diffusion processes, and in many cases it is now possible to predict the performance

of or "design" porous electrodes (Ref. 3), such design being directed towards the maximization of electrode performance through suitable compromise between the different geometric and materials variables and the multiple functions that the electrode must serve.

Specifically, the present system separates the gas dissolution process from the electrode, as in the scheme shown in Figure 1. A cursory glance at such a system may result in dismissing it as apparently complex and bulky. A quantitative estimate of the component's dimensions, however, shows that with proper design this is not the case.

The system consists of two liquid loops where the electrolyte, containing the respective reactants in solution, is forced through electrodes in which a large fraction of the reactants is depleted. The electrolyte is then recirculated through the respective liquid-gas contactors, where the reactant gases from the storage containers are dissolved, "recharging" the electrolyte. The heat generated at the electrodes is dissipated in part at the radiator and in part, as latent heat, in the evaporator.

Electrode material and structure can be designed so that mass transfer occurs from the bulk liquid to the total active electrode surface so that the electrochemical process is not so localized. The parameters influencing such an optimization are:

1. The catalytic area participating in the reaction.

2. The mass transfer from the bulk fluid to such area.

3. The ohmic drops through electrode material and electolyte.

4. Pressure drops (parasitic power requirements).

Similarly, the saturators can be designed specifically for their function, now independent of the electrode process, providing a suitable compromise between gas-liquid contact area and pressure drops.

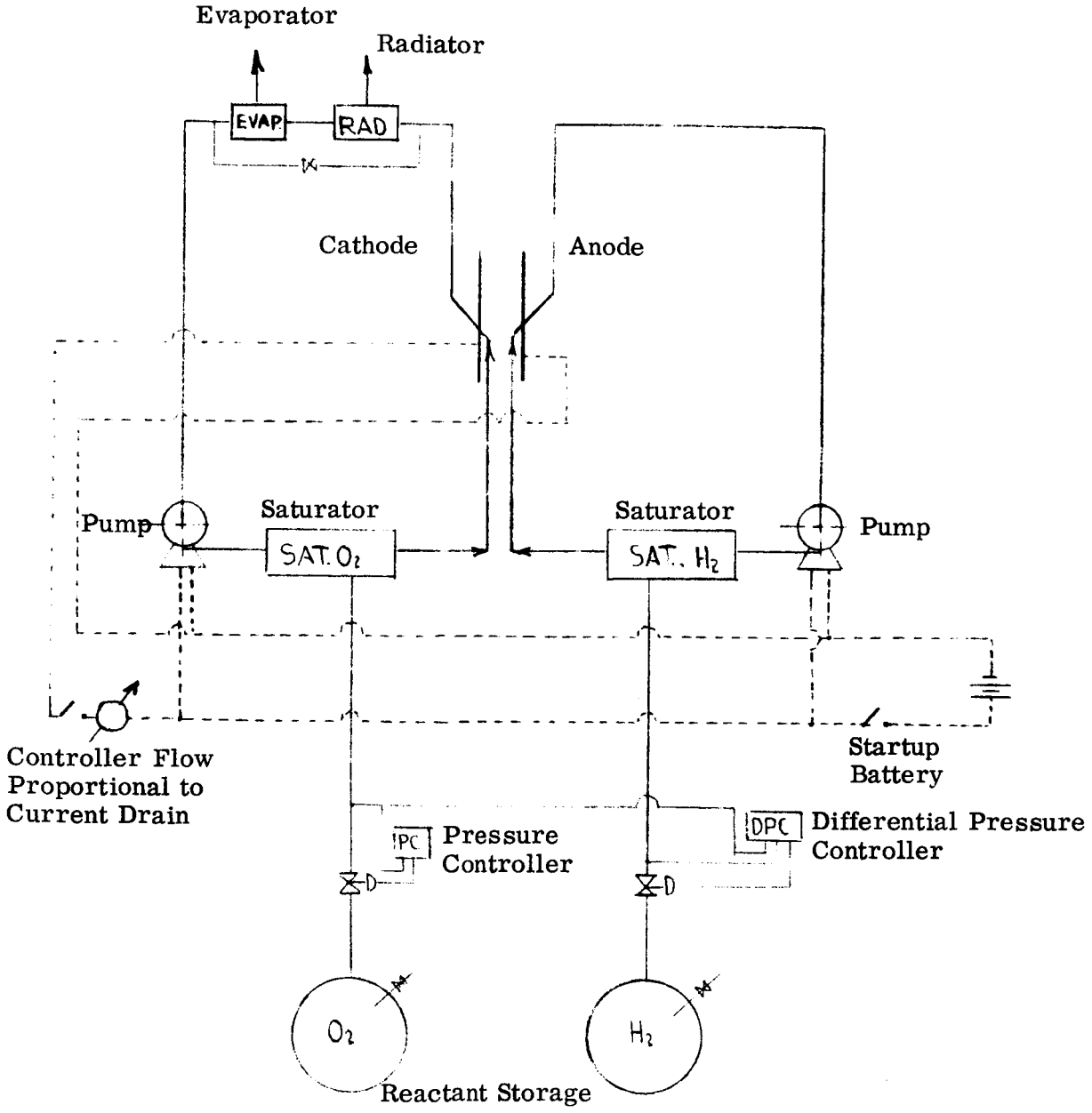

Figure 1. Flow Diagram, Flow Through Electrode Fuel Cell

The physical model adopted for this study is presented in Section 3, with comments on specific assumptions and design decisions. A mathematical model of the total system was constructed and a multi-variate optimization program was utilized to calculate the minimum system weight with respect to the following optimizable quantities:

1. Current Density at Geometric Electrode Area. Geometric electrode area is defined as the projected area of the electrode at the two electrode interfaces.

2. Maximum Local Current Density at Oxygen Electrode. (Based on the internal or micropore area of the structure.)

3. Oxygen Electrode Pore Size.

4. Hydrogen Electrode Pore Size.

5. Hydrogen Electrode Through Electrolyte Flow.

Such an optimization was carried out for a variety of cases, where the following conditions were explored:

1. Mission Length (5 hours to 10 days)

2. Saturator Pressure (5 atm to 50 atm)

3. System Operating Temperature (20° C to 100°C)

4. Oxygen Electro-Catalyst (Pt or Ag)

The results for the optimized system are presented and discussed in Section 5.

Diagrams of the electrode arrangement for the fuel-cell stack and the proposed electrolyte manifolding to minimize power drain by short circuiting through the electrolyte are shown in Section 6 of Appendix A.

Section 3

SYSTEM WEIGHT CALCULATIONS AND OPTIMIZATION PROGRAM

3.1 System Weight Calculations

A 1.0 kw net output was taken as the design basis. It was found from preliminary calculations that the components of a system with this power output would be of such dimensions that scaling down to a net output of about 500 watts or up to 5 kw could be carried out in essentially linear fashion.

This direct proportionality between system weight and net power output stems from the fact that the main weight components, except for reactant storage, are made up of modular elements used in quantity.

The total system weight was computed as the sum of the main component weights:

$$\text{Total Wt.} = \text{Wt } O_2 \text{ electrode} + \text{Wt } H_2 \text{ electrode} + \text{Wt Radiator} + \text{Wt reactants} + \text{Wt tanks} + \text{Wt } O_2 \text{ saturator} + \text{Wt } H_2 \text{ saturator}.$$

For the case of the electrodes and saturators, a factor was taken to account for framing, enclosure, manifolds and ducting. With proper design, however, it was found that these factors were relatively small, and thus an exact value was not necessary to predict the total system weight with an accuracy of ten percent or better. The effects of system pressure drop, electrode overvoltage and IR losses all automatically become part of the fuel and tankage weight penalty with the system weight calculation procedure used, which takes a 1.0 kw net output as the design basis. The derivation of some of the basic performance and weight equations for the critical components, including comments on the design concept and assumptions made, are presented in Appendix A.

The compilation for the calculated system weight and performance subroutine is included in Appendix B. The computer printout for a typical case is shown in Appendix C.

3.2 Optimization Program

This section describes the computer optimization procedure used. Briefly stated, the optimization consisted of calculating the total system weight for a given set of input weight data while varying system parameters systematically until a minimum system weight is obtained.

Minimum weight and optimum design are clearly dependent on the values of the unit weights assigned to the various components.

The inputs for optimization are the unit weights of the various components, while the outputs are the minimum system weight and the optimum design. The performance equations relate the system parameters, and the optimization sequence compare the system weights for different configurations and selects the output for minimum weight. The optimization sequence for a system with n optimizable quantities X_1, Y_1, Z_1, etc., is the following:

1. Define an increment for each parameter.

2. Start, compute the system weight for the initial values of the n parameters.

3. Take the X parameter, add the first increment and compute the weight. If the new weight is less, use the new value X_2 and add another increment, minimizing the weight with increasing X until the final weight begins to rise or a limit is reached. Take the final increment, divide it by 20 and decrease until the weight begins to rise. Stop.

4. Keep the final value of X, begin the same procedure adding increments to Y until the new minimum weight is reached. Repeat this procedure for the n quantities.

5. Repeat the cycle starting again with X until the final minima are reached.

This procedure is not effective for reaching a true minimum for some cases when the total weight surface has double or multiple minima, such as a saddle surface.

Section 4

RESULTS

A summary of computed system weights is shown in Figure 2 in the form of specific energy density as a function of mission length. For long missions, the weight is mostly that of the reactants as the weight breakdown curves of Figures 3, 4, and 5 indicate. For shorter missions, of the order of five hours to one day, the weights of the different components are of comparable magnitude. The system weight decreases as the operating pressure is raised, since higher pressure allows higher electrode current densities, faster mass transfer in the saturators and lower pumping power. Beyond 20 atmospheres, however, the weights approach asymptotic limits so fast that there is no point in considering the pressure increases beyond 50 atmospheres at practical current densities. A silver catalyst at the oxygen electrode results in a lower operating voltage than the use of platinum, and this is reflected in the considerably higher total system weight due to the higher reactant consumption.

For a five-hour mission, specific energy outputs of 100-150 watt-hours per pound are predicted. These figures increase to 300-500 watt-hours per pound and over for mission lengths of one day and more.

The weight breakdown curves of Figures 3, 4, and 5 show that the individual component weight stays about constant for the optimized system, almost independent of mission length.

At first glance such a result appears surprising, since one would expect a trade-off between equipment size and efficiency (larger equipment size, higher efficiency for long missions). In fact, the efficiency is almost at its possible maximum in all cases, as shown in Figure 6 for the variation of current density and operating voltage with mission length. Higher current densities decrease the electrode size, but increase reactant and tankage weights; furthermore, the added inefficiency increases the radiator, saturator and pumping requirements as well. The result is a flat plateau around the optimum design.

Figure 7 shows the effect of electrode current density on system weight for a system purposely designed to operate at a current density different than the optimum. It is evident that the final system weight is relatively insensitive to current density, since a variation from 0.15 to 0.40 amperes/cm^2 does not change the final energy density by more than ten percent. The presence of double maxima and the relative flatness of the curves explain why one case presented in Figure 6 (100°C, 50 atm) seems to optimize at higher current densities with longer mission length. The optimization program most probably became "stuck" on a double minima at the higher current density range. The effect on the final system weights, however, is small.

The computed parasitic power consumption remains essentially constant with mission length for all cases, as shown in Figure 8. This finding is accounted for by the fact that the main pressure drop is found at the saturators, where the electrolyte flows through a 5 cm length of porous material, compared with a fraction of a millimeter for thickness of the electrodes. The parasitic power (pumping power) requirement is therefore proportional to the total liquid circulation rate and inversely proportional to viscosity. Since electrolyte viscosity and reactant solubility decrease (flow rate increases) with a temperature increase, the effects are partially compensating. A higher total system pressure, however, results in lower parasitic power requirements, and it is clear that system pressures of 5 atm or lower result in excessive pumping penalties.

In this design, no allowance was made for internal losses introduced by short-circuiting of the electrodes stacked in series through the electrolyte. It was decided, after order of magnitude calculations, that proper manifolding of the electrolyte can result in long and narrow electrolyte paths, through which less than one or two percent of the total power is dissipated, even when the cells are stacked for 12 or 28 volt per stack.

Overall system performance was calculated with confidence, since all kinetic and mass transfer input data have an experimental basis. The performance of such high current-density flow-through electrodes, however, should be confirmed experimentally, since the calculations are based on simplified, idealized structures.

The performance of the saturators needs experimental confirmation as well, not as much in terms of achievable mass-transfer rates as to ascertain whether any flow or side leakage problems are encountered with such controlled wetting structures.

Since, in all cases, the full power parasitic power demands are low, the system can be easily started and restarted, even when the reactants have been depleted near the electrode region, by the use of either a rechargeable or non-rechargeable battery. The total start-up power demand will not exceed more than 20% of the full power parasitic power demand (or about 20 watts per kw of system output) and should not last for more than a few seconds, before the reactants are brought from the saturators to the electrodes.

A control system will be needed to regulate the electrolyte circulation rate in proportion to the total power demand (output current). All of the components, both active and passive, should be able to withstand a service life in excess of 3000 hours. The only components that would require exhaustive life testing, since no operating experience is presently available, are the saturators. Particular attention should be given to the stability of the controlled wetting structures, and to the effects of any impurities introduced with the reactants or leached out of exposed components.

SPECIFIC ENERGY OUTPUT VS. MISSION LENGTH

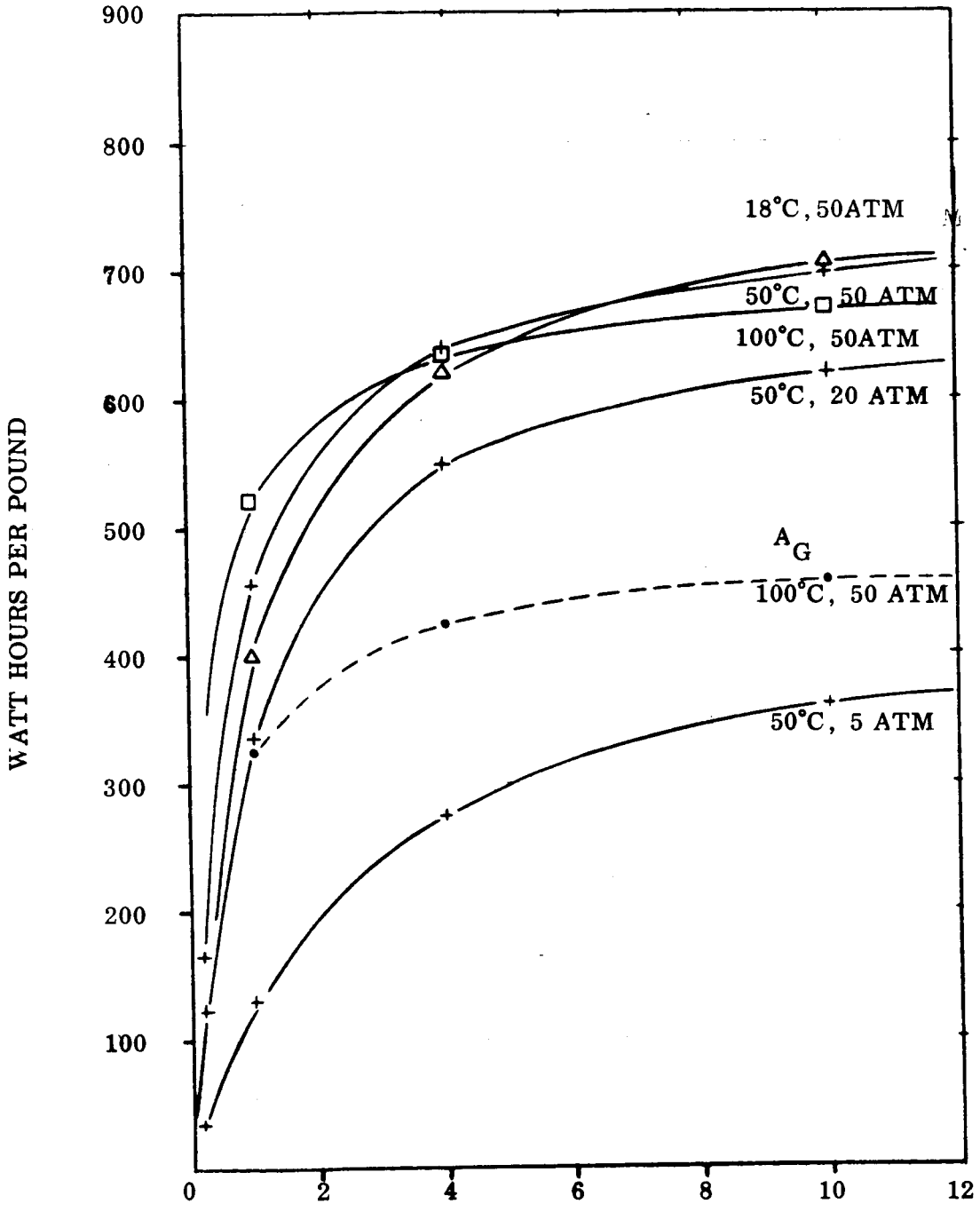

Figure 2

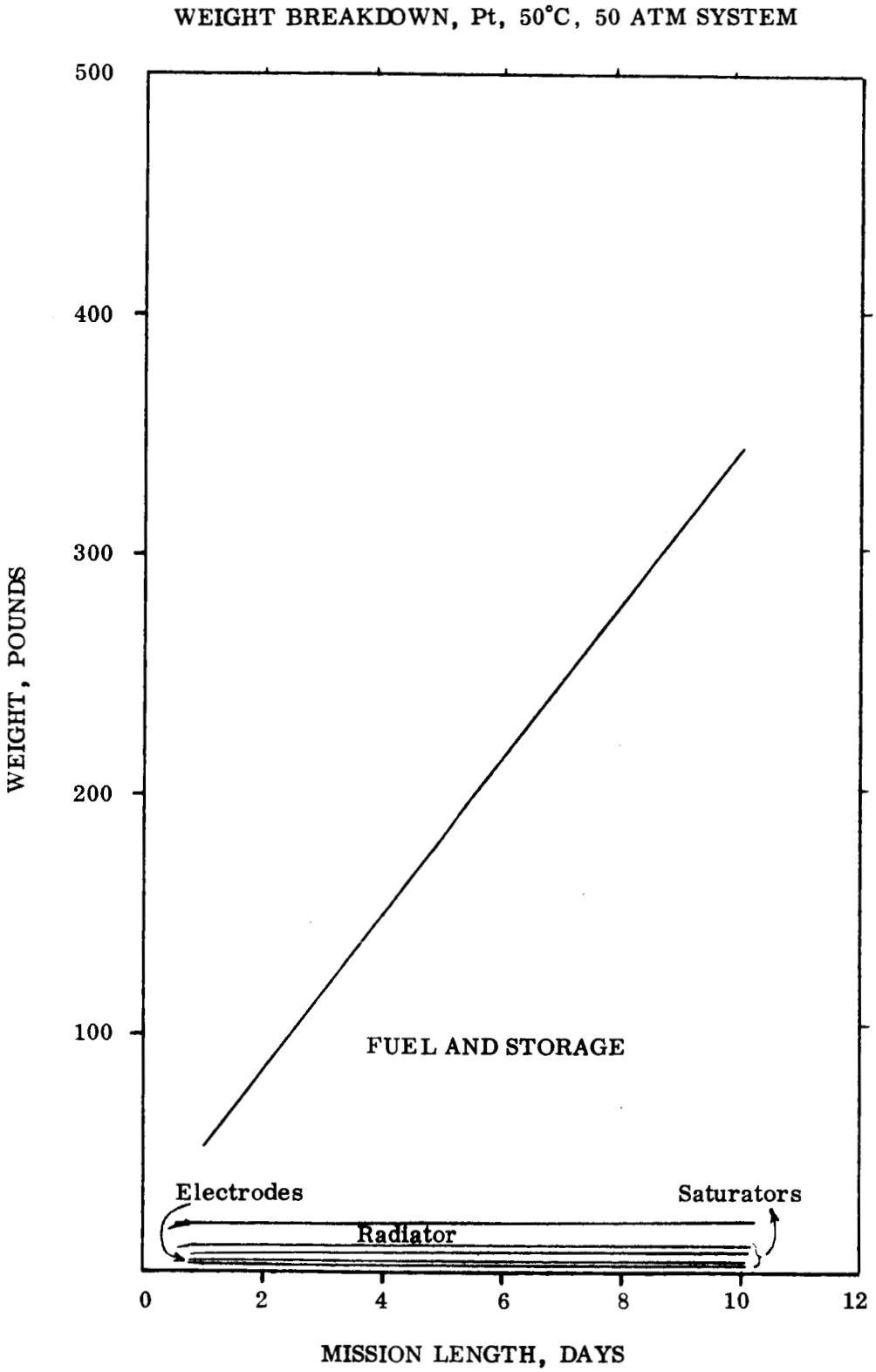
WEIGHT BREAKDOWN, Pt, 50°C, 50 ATM SYSTEM
500
400
300
200
100
WEIGHT, POUNDS
FUEL AND STORAGE
Electrodes
Saturators
Radiator
0
2
4
6
8
10
12
MISSION LENGTH, DAYS

Figure 3

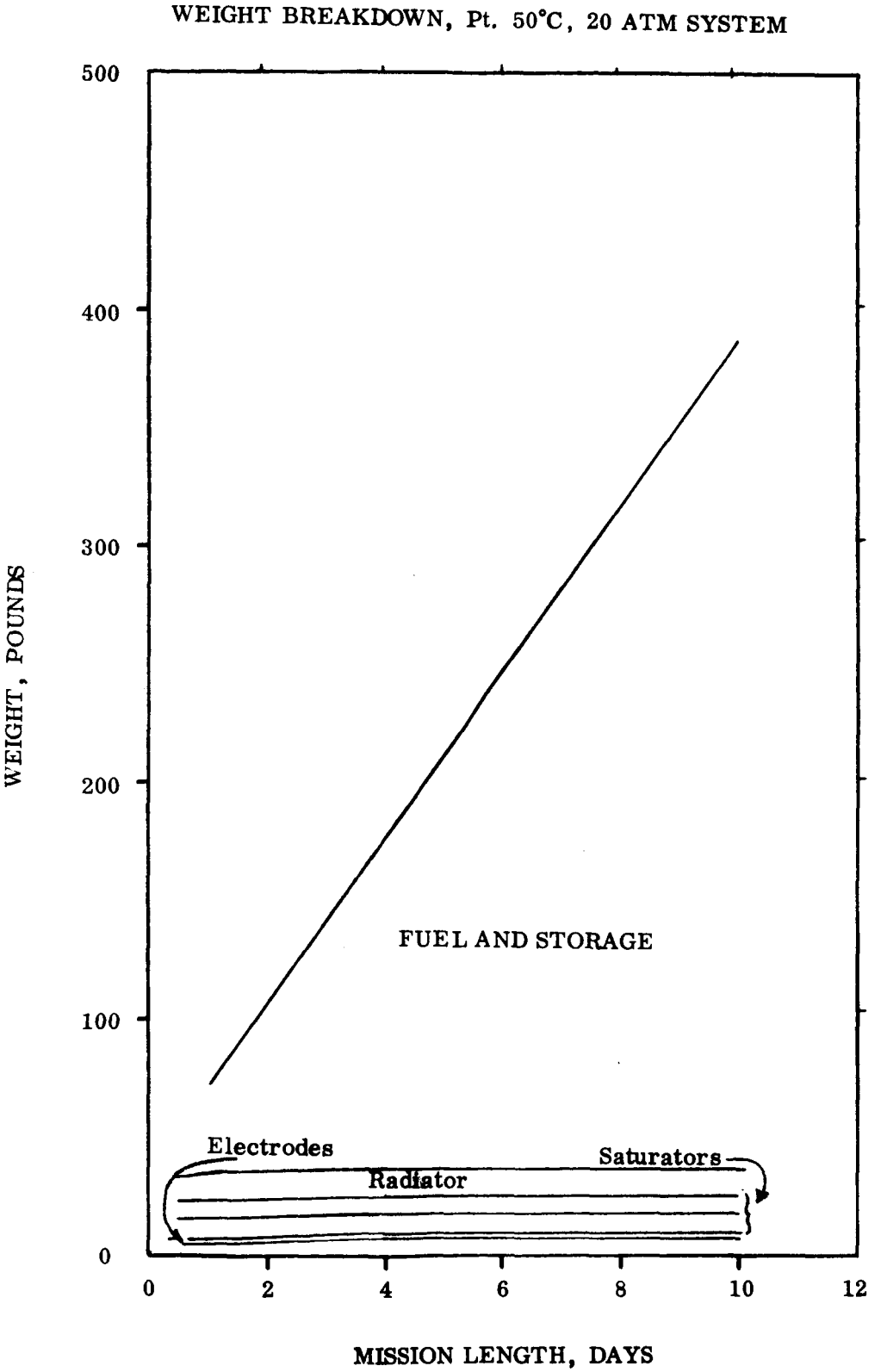
WEIGHT BREAKDOWN, Pt. 50°C, 20 ATM SYSTEM
WEIGHT, POUNDS
500
400
300
200
100
0
FUEL AND STORAGE
Electrodes
Saturators
Radiator
0
2
4
6
8
10
12
MISSION LENGTH, DAYS

Figure 4

WEIGHT BREAKDOWN, Pt. 50°C, 5 ATM SYSTEM

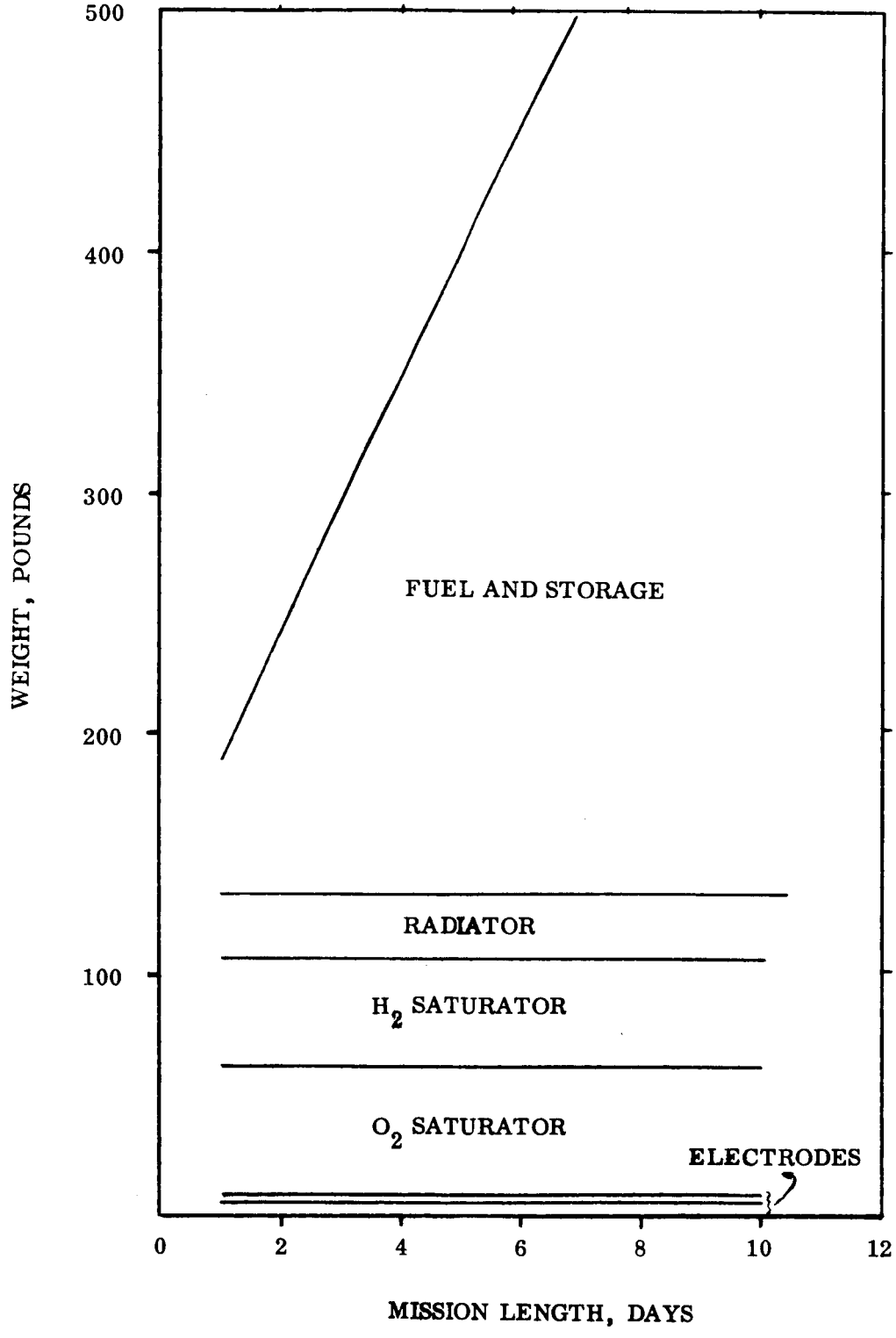

Figure 5

OPTIMIZED CELL VOLTAGE AND CURRENT DENSITY VS. MISSION LENGTH

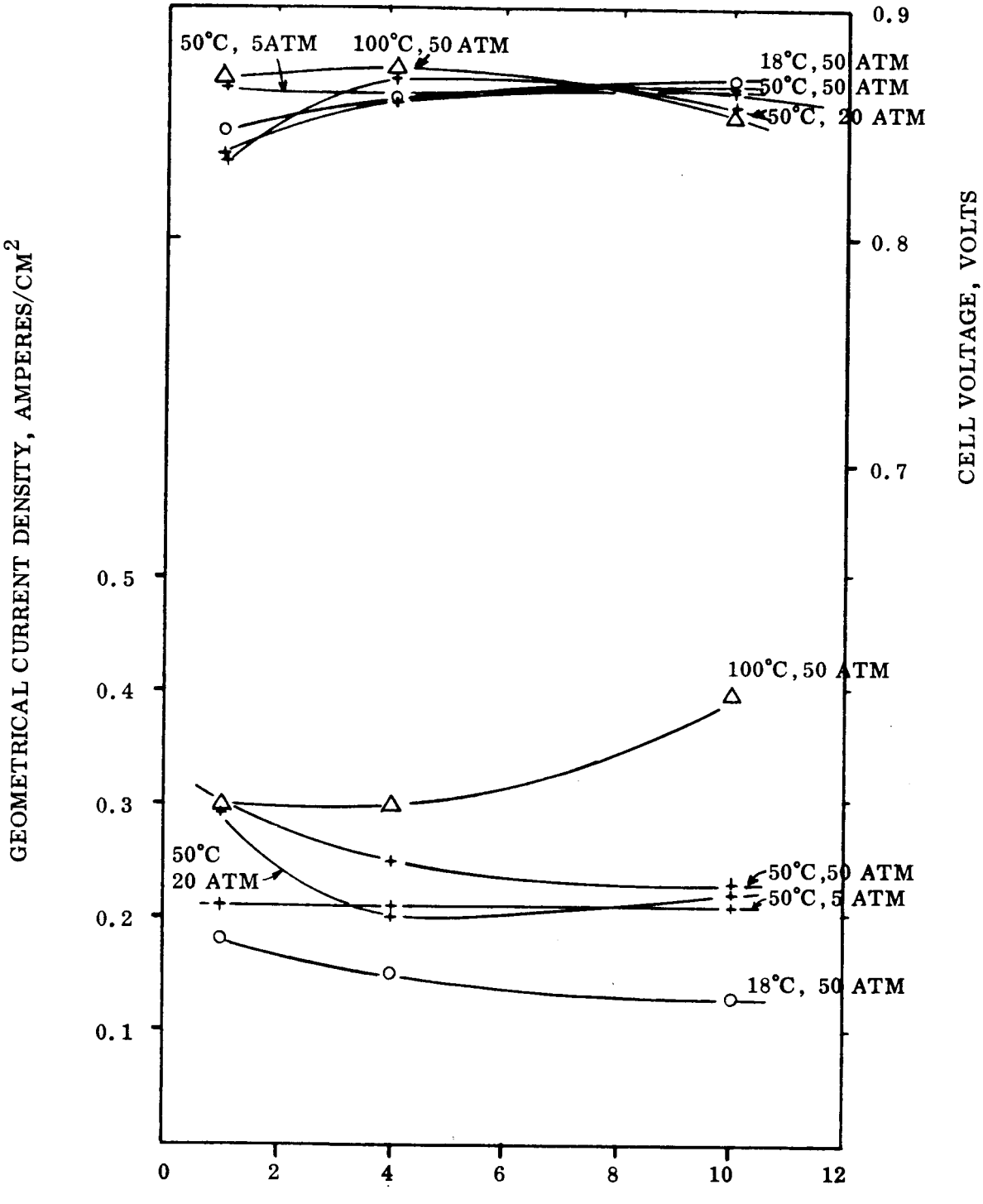

Figure 6

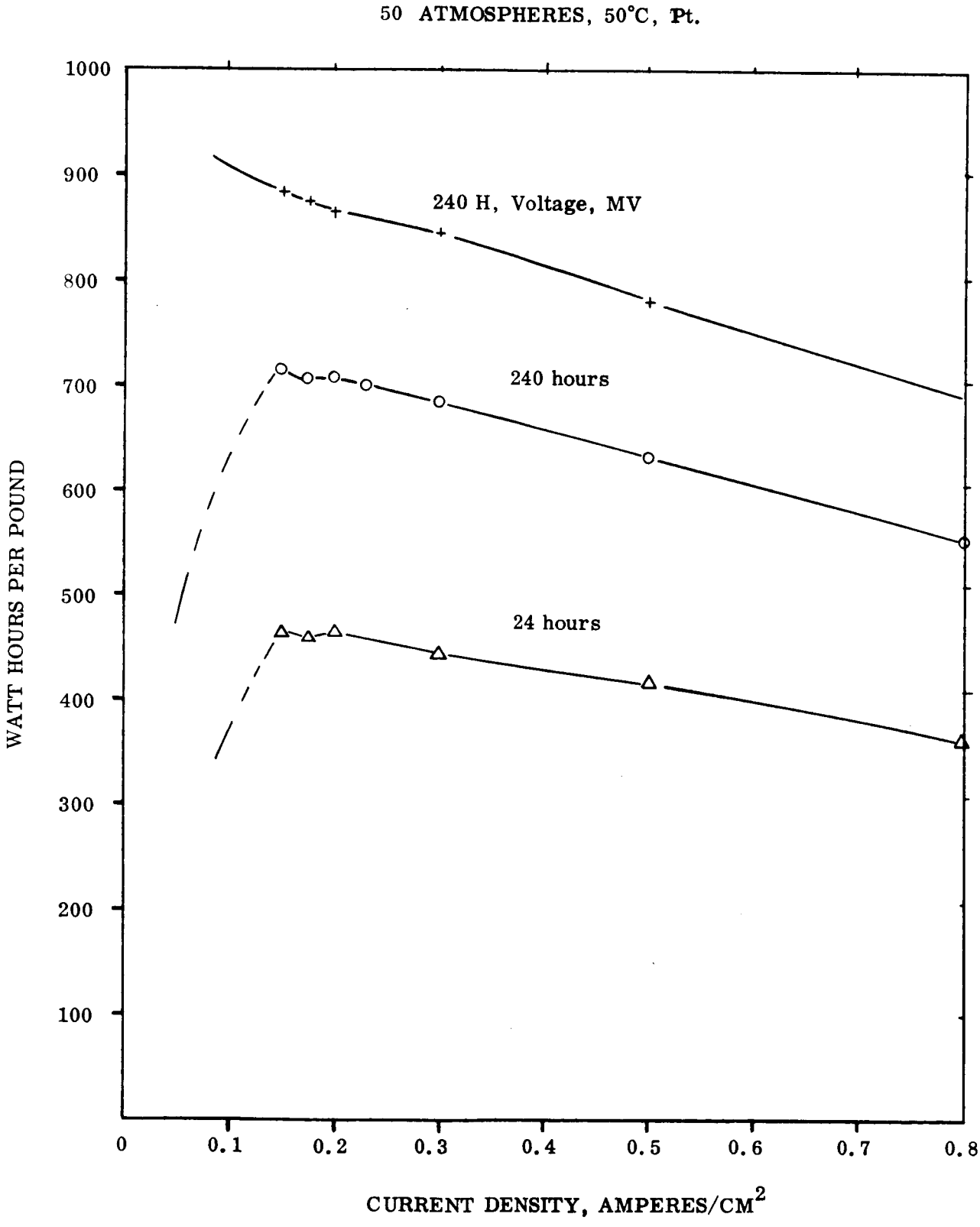
50 ATMOSPHERES, 50°C, Pt.
1000
900
800
700
600
500
400
300
200
100
240 H, Voltage, MV
240 hours
24 hours
WATT HOURS PER POUND
0
0.1
0.2
0.3
0.4
0.5
0.6
0.7
0.8
CURRENT DENSITY, AMPERES/CM2

Figure 7

Total Parasitic Power Demand for Different Systems

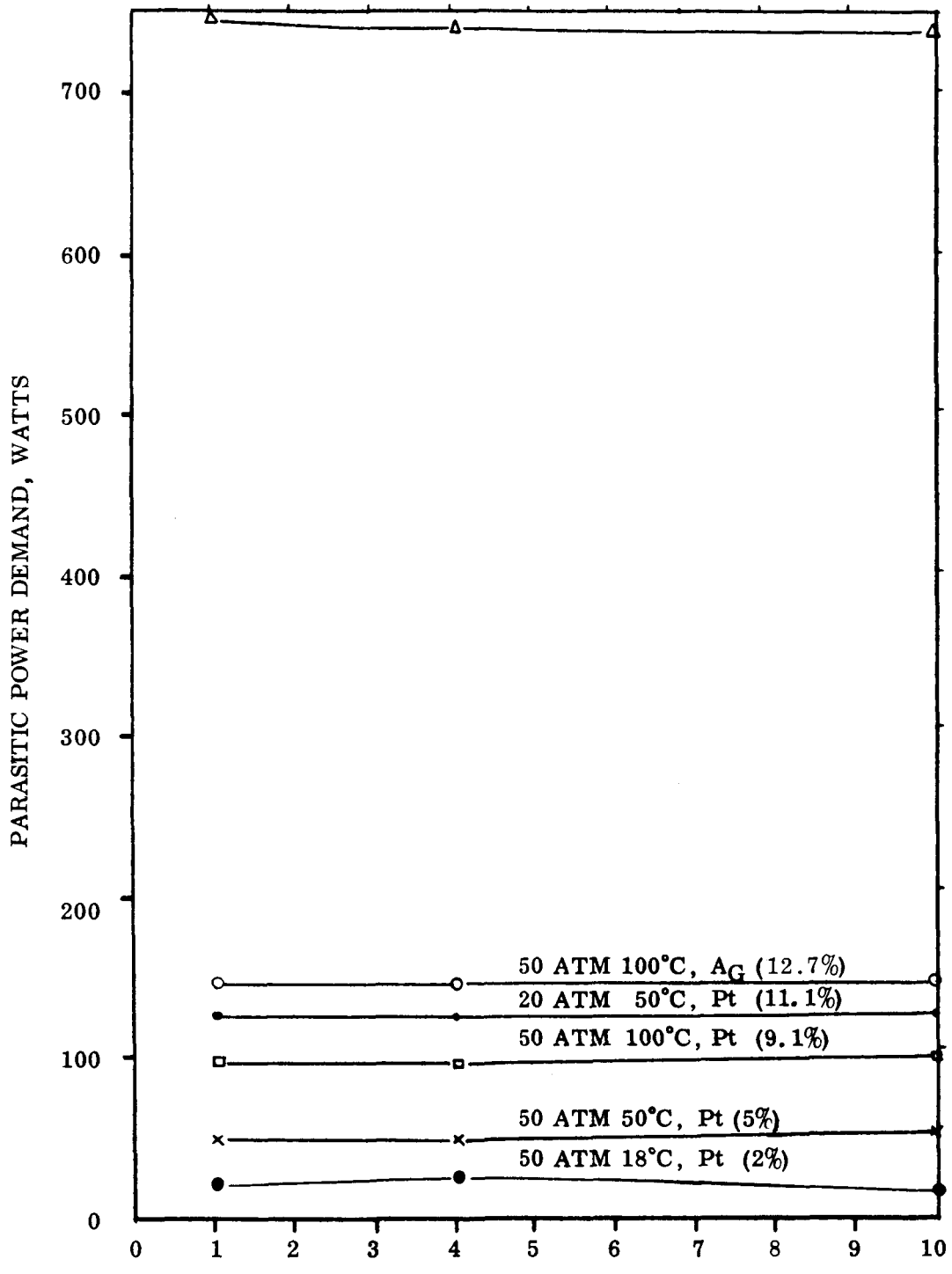

Figure 8

Section 5

LIST OF REFERENCES

1. Reti, A. R., "Rate Limiting Steps on Fuel-Cell Electrodes," ASD-TDR-63-118.

2. Meissner, H. P. and Reti, A. R., "Fuel Cells Using Flooded-Flow Electrodes," ASME Paper No. 63-WA-350.

3. Meissner, H. P. and Reti, A. R., "Predicted Performance of Air Electrodes," published in "Fuel Cells," Chemical Engineering Progress Technical Manual, New York, 1963, p. 40-44.

4. D'Ambrosio, B., "Polarization Study of the Hydrogen Flow Through Electrode," Ph. D. Thesis in Chemical Engineering, Worcester Polytechnic Institute, 1965.

Appendix A

BASIS FOR DESIGN AND WEIGHT EQUATIONS

A.1 Oxygen Electrode Design

Assume a structure of parallel cylindrical pores such as in Figure A1, where the oxygen saturated electrolyte enters the pore at x = 0. Assume the reaction to be kinetically controlled. Actual kinetics measured experimentally and described by the Tafel equation (Ref. 1) are used in this calculation.

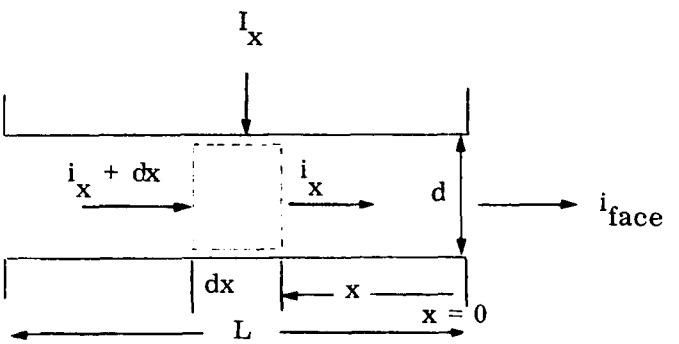

Figure A1

The electrode weights were computed from the total electrode area required, the thickness, electrolyte and separator layer thickness plus a factor for framing, ducting and containment.

$$V_{x+dx} - V_x = i_x \frac{4\rho}{\pi d^2} dx$$

and

$$\frac{d^2 V}{dx^2} = \frac{4\rho}{\pi d^2} \frac{di}{dx}$$

From the Tafel equation, one can relate I and V,

where: V_x - electrode voltage at position x in the pore, volts

i_{face} - geometrical electrode current density, amperes/cm^2

x - distance from along the pore from the electrode face, cm

L - pore length, cm

ρ - electrolyte resistivity, ohms-cm

d - pore diameter, cm

I - local current density, based on catalyst surface, amperes/cm^2

Using the convention chosen here, as V is raised, I is decreased and so the slope of V versus I is negative

$$V = a - \frac{b}{2.3} \log_e I$$

and so

$$I = e^{-(2.3/b)(V - a)}$$

i.e.,

$$\frac{d^2V}{dx^2} = - \frac{4\rho}{d} e^{-(2.3/b)(V - a)}$$

Put

$$\frac{dV}{dx} = i \frac{4\rho}{\pi d^2}$$

$$\frac{d^2V}{dx^2} = \left(\frac{4\rho}{d^2}\right)^2 i \frac{di}{dV}$$

or

$$\left(\frac{4\rho}{\pi d^2}\right)^2 \frac{i^2}{2} = + \frac{4\rho}{d} \cdot \frac{b}{2.3} e^{-(2.3/b)(V - a)} + C_1$$

$$\left(\frac{4\rho}{\pi d^2}\right)^2 \frac{i^2}{2} = \frac{4\rho b}{2.3d} I + C_1$$

at $x = 0$ $I = I_o$ and $i = i_o$

$$\therefore \quad C_1 = \left(\frac{4\rho}{\pi d^2}\right)^2 \frac{i_o^2}{2} - \frac{4\rho b}{2.3d} I_o$$

and so
$$\frac{4\rho}{\pi d^2} i = + \sqrt{\frac{8\rho b}{2.3d} I + 2C_\rho}$$

i.e.,
$$= \frac{dV}{dx} = -\frac{b}{2.3} \frac{dI}{Idx}$$

$C_1 < 0$ is the only possible case.

i.e.,
$$\frac{4\rho i_o}{\pi d^2} < \sqrt{\frac{8\rho b}{2.3d} I_o}$$

The differential equation is:

$$-\frac{b}{2.3} \int \frac{dI}{I\sqrt{\frac{8\rho b}{2.3d} I + 2C_1}} = \int dx$$

with b positive

i.e.,
$$-\frac{b}{2.3} \frac{2}{\sqrt{-2C_1}} \tan^{-1}\sqrt{\frac{\frac{8\rho bI}{2.3d} + 2C_1}{-2C_1}} = x + C_2$$

and at $x = 0 \quad I = I_o$.

$$C_2 = -\frac{b}{2.3}\,\frac{2}{\sqrt{-2C_1}}\,\tan^{-1}\sqrt{\frac{\frac{8\rho b I}{2.3d} + 2C_1}{-2C_1}}$$

$$= -\frac{b}{2.3}\,\frac{2}{\sqrt{-2C_1}}\,\tan^{-1}\sqrt{\frac{\left(\frac{4\rho}{\pi d^2}\right)^2 i_o^{\,2}}{-2C_1}}$$

and

$$\sqrt{\frac{\frac{8\rho b I}{2.3d} + 2C_1}{-2C_1}} = \tan\frac{2.3\sqrt{-2C_1}}{-2b}\,(x + C_2)$$

$$I = \frac{(2.3d)(-2C_1)}{8\rho b}\left[\tan^2\frac{2.3\sqrt{-2C_1}}{-2b}\,(x + C_2) + 1\right]$$

$$I = \frac{(2.3d)(-2C_1)}{8\rho b}\,\sec^2\left[\frac{2.3\sqrt{-2C_1}}{-2b}(x + C_2)\right]$$

$$\int_{i_o}^{i} di = -\int_{x=0}^{x} \pi d I\, dx$$

$$i - i_o = -\frac{\pi d^2\sqrt{-2C_1}}{8\rho}\left[\frac{8\rho\, i_o}{\pi d^2\sqrt{-2C_1}} - \frac{\tan 2.3\sqrt{-2C_1}}{-b}\,(x + C_2)\right]$$

For $i = 0$

$$L = \frac{b}{2.3} \frac{2}{\sqrt{-2C_1}} \tan^{-1} \frac{4\rho\, i_o}{\pi d^2 \sqrt{-2C_1}}$$

Limit as $i_o \rightarrow 0$

$$L = \frac{b2}{2.3\sqrt{-2C_1}} \cdot \frac{4\rho\, i_o}{\pi d^2 \sqrt{-2C_1}}$$

$$2C_1 = \left(\frac{4}{\pi d^2}\right)^2 i_o^2 - \frac{2 \times 4\rho b}{2.3d} I_o$$

$$= \left(\frac{9\rho\, i_{face/cm^2}}{\pi}\right)^2 - \frac{8\rho b}{2.3d} I_o$$

if $2C_1 \geq 0$

then it is impossible to operate the cell (> 0), or an infinite length is required (= 0).

If $2C_1 < 0$, then

$$L = \frac{b}{2.3} \frac{2}{\sqrt{-2C_1}} \tan^{-1} \frac{9\rho\, i_{face/cm^2}}{\pi \sqrt{-2C_1}}$$

A.2 Hydrogen Electrode Design

Experimental data (Refs. 1 and 5) indicate that the electrode kinetics does not limit the hydrogen electrode (the exchange current density has been measured to be about 1 mA/cm^2), because rough, high surface-area (platinum black coated) internal surfaces can be used. The hydrogen flow-through electrode is, therefore, liquid phase mass transfer controlled and the necessary electrode thickness (pore length) and internal voltage drop can be calculated according to the following derivation:

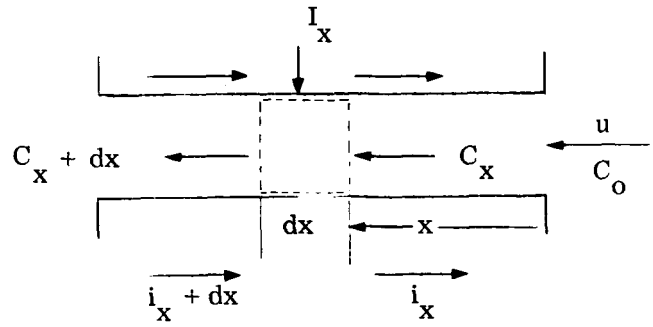

Figure A2

Material balance around an element dx within the pore

$$\frac{\pi d^2 u}{4} \cdot \frac{dC_x}{dx} \cdot dx = \pi d \cdot \frac{dx\, I_x}{2F}$$

$$\left(\frac{2Fud}{2}\right) \frac{dC_x}{dx} = I_x.$$

To estimate (dC_x/dx)

If K based on average cross-sectional concentration

$$-\frac{u\pi d^2}{4} C_{x+dx} + \frac{u\pi d^2}{4} C_x = K \cdot \pi d \cdot dx\, C_x$$

or

$$-\frac{du}{4} \frac{d(C_x)}{dx} = K C_x$$

where:

X	-	distance along pore length from electrode surface, cm
C	-	hydrogen concentration in electrolyte, gram moles/cm^3
u	-	electrolyte velocity, cm/sec
I	-	local current density, based on catalyst surface, amperes/cm^2
i	-	geometrical current density, amperes/cm^2
d	-	pore diameter, cm
F	-	Faraday's constant, 96,500 coulombs/gram equivalent

K - mass transfer coefficient, cm/sec

ρ - electrolyte resistivity, ohms-cm

ΔV - voltage drop inside the pore, volts

L - pore length, cm

$$-\frac{dC_x}{C_x\,dx} = \frac{4K}{ud}$$

i.e.,

$$-\int_{C_x=C_{x=0}}^{C_x} d\ell n\, C_x = \int_{x=0}^{x} \frac{4K}{ud}\,dx$$

$$\ell n \frac{C_x}{C_{x=0}} = -\frac{4K}{ud}\,x$$

or

$$C_x = C_{x=0}\, e^{-(4K/ud)\,x}$$

Total current i_o in amperes/pore is given by:

$$i_o = (C_{x=0} - C_{x=L})\frac{\pi d^2}{4}\,u \cdot 2F$$

and

$$C_{x=L} = C_{x=0}\, e^{-(4K/ud)\,L}$$

so

$$i_o = \left(\frac{\pi d^2 u\, 2F}{4}\right) C_{x=0}\,(1-e^{-(4K/ud)\,L})$$

or

$$1 - e^{-(4K/ud)\,L} = \frac{4i_o}{\pi d^2 u\, 2F\, C_{x=0}}$$

$$L = -\frac{ud}{4K}\,\ell n\left[1 - \frac{4\,i_o}{\pi d^2 u\; 2F C_{x=0}}\right]$$

and since $i_o = 2.25\, d^2\, i_{face}$

$$L = -\frac{ud}{4K}\,\ell n\left[1 - \frac{9\,i_{face}}{\pi u\, 2F\, C_{x=0}}\right]$$

Calculation of Potential Drop

$$dV_x = \frac{i_x\, 4\rho}{\pi\, d^2}\, dx$$

and

$$di_x = \frac{\pi d^2}{4}\, u \cdot 2F\, dC_x$$

so

$$i_x = \frac{\pi\, d^2\, u \cdot 2F}{4}\,(C_x - C_{x=L})$$

$$= \frac{\pi d^2\, u\, 2F}{4}\left[C_{x=0}\, e^{-(4K/ud)x} - C_{x=0}\, e^{-(4K/ud)L}\right]$$

and so

$$\Delta V = \frac{4\rho}{\pi d^2} \cdot \frac{\pi d^2\, u\, 2F}{4}\, C_{x=0} \int_{x=0}^{x=L} \left(e^{-(4K/ud)x} - e^{-(4K/ud)L}\right) dx$$

$$= 2Fu\rho\, C_{x=0} \left\{\left[-\frac{ud}{4K}\, e^{-(4K/ud)x}\Big|_{x=0}^{x=L} - Le^{-(4K/ud)L}\right]\right\}$$

$$= 2F \quad u\, C_{x=0} \left[\frac{ud}{4K} - \frac{ud}{4K} e^{-(4K/ud)L} - Le^{-(4K/ud)L} \right]$$

$$\Delta V = 2F\rho\, u\, C_{x=0} \left[\frac{ud}{4K} - e^{-(4K/ud)L} \left(\frac{ud}{4K} - L \right) \right]$$

$$= 2F\rho\, u\, C_{x=0} \left[\frac{ud}{4K} (1 - e^{-(4K/ud)L}) + Le^{-(4K/ud)L} \right]$$

A.3 Radiator Weight Estimate

For mission lengths over 4 hours, it is advantageous to reject heat by means of a radiator. For shorter term missions it becomes simpler and lighter to carry some excess water to satisfy the evaporative cooling requirements.

The total radiator required was estimated on the basis of a specific radiator weight of 1 lb/ft^2 (standard practice) and assuming heat is radiated to outer space with a view factor of one. The total amount of heat to be rejected per unit time is Q = (lb H_2 consumed/hr) (enthalpy of combustion, kw/lb) - 1.0 kw, or the total heat generated minus the net power withdrawn.

A.4 Saturator Design and Weight Estimate

The saturators were designed on the basis of a configuration consisting of multiple layers of wetting (i.e., porous stainless steel or nickel) and non-wetting (i.e., porous teflon) materials. These layers can be as thin as 0.010", and are present state-of-the-art structures that can be purchased or manufactured. A saturator exit concentration of a certain fraction of the equilibrium concentration (0.9) was assumed in all cases. A liquid phase diffusion path lengthof 1/4 of the wetted layer thickness was taken for all calculations. The total interfacial saturator area could then be calculated; for example, in the case of the oxygen saturator:

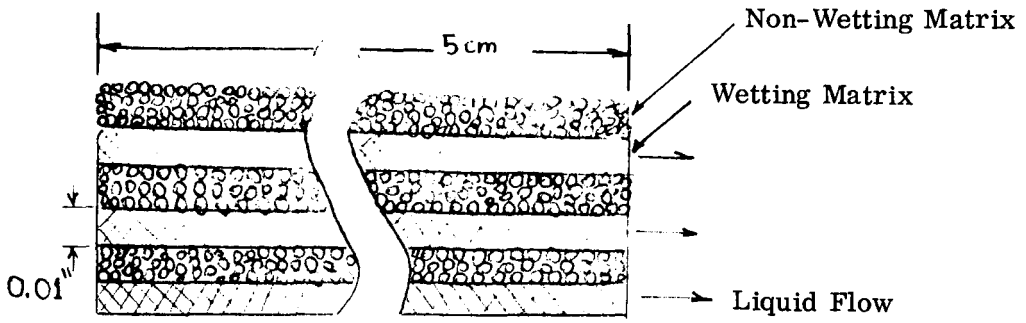

Figure A.4.1 Saturator Structure

$$A_{interfacial} = \frac{A_{face} \times i \times L/4}{4\,F\,(C_{in} - C_{out})} \ln\left[\frac{C_{eq} - C_{out}}{C_{eq} - C_{in}}\right]$$

In this case all concentrations refer to oxygen. The saturator weight was then computed based on the interfacial area and the thickness and density of both gas and liquid layers.

A.5 Reactant and Tankage Weight Estimates

Reactant consumption rate is given by total electrode area times the current density (negligible catalytic recombination after diffusion through the separators is assumed). Since this system appears attractive only at fairly high operating pressures (10 - 50 atm), supercritical cryogenic storage was considered when evaluating tank weights. The tank weight is proportional to the volume of reactant to be stored, but the proportionality factor decreases as tank size increases. For the purpose of these calculations, where the amounts to be stored are small, the tank weight was assumed to be 0.5 lb/lb reactants. This figure checks approximately with Bendix data for supercritical storage of LOX. This simplification results in tankage weight estimates which are about 20% too low compared with the accepted tankage weights of 2.5 - 3.3 lb/lb stored hydrogen and 0.29 - 0.33 lb/lb stored oxygen. These numbers are for 20 - 30 lbs of hydrogen and eight times as much oxygen. The present analysis considered total reactant weights in the 30 to 500 lb range.

A. 6 Electrode Arrangement

The electrodes were assumed to be stacked in a fashion such as shown in the sketches below. The top view of the flow-through electrode stack shows the anode and cathode separated by a corrugated separator membrane. The total gap between electrode surfaces is 2 mm. Manifolds at the top and bottom of the stacks keep the streams from mixing.

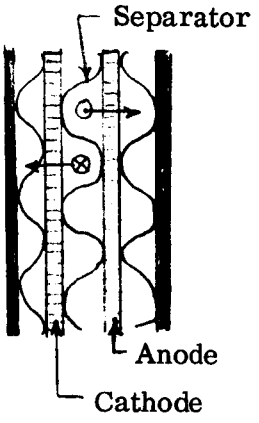

Figure A.6.1 Electrode Arrangement, Top View

The incoming or outgoing streams are manifolded in parallel into several electrodes which are electrically connected series. The electrical leakage through these electrolyte paths is minimized by creating long and narrow paths for current flow from electrode to electrode, as shown in the side view of the stacks.

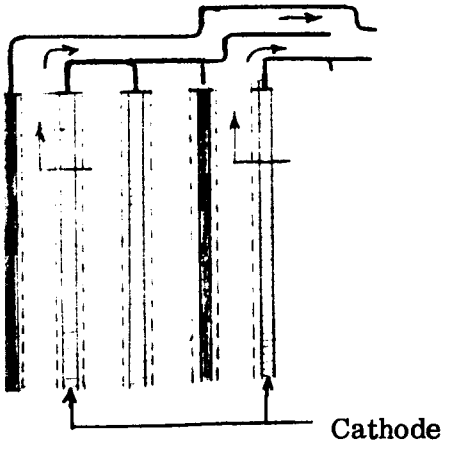

Figure A.6.2 Electrode Arrangement, Side View

Appendix B

SYSTEM PERFORMANCE AND WEIGHT SUBROUTINE

FORTRAN NOMENCLATURE

CFACE:	Current density for geometric electrode area, amperes/cm^2
CLOC:	Oxygen electrode local (based on internal area) current density, amperes/cm^2
DO2:	Oxygen electrode pore diameter, cm
VH2:	Electrolyte velocity through the hydrogen electrode, cm/sec
DH2:	Hydrogen electrode pore diameter, cm
TIME:	Mission length, hours
XLO2:	Oxygen electrode thickness, cm
XLH2:	Hydrogen electrode thickness, cm
AFACE:	Electrode face area, cm^2
ASATO:	Oxygen saturator gas-liquid interfacial area, cm^2
ASATH:	Hydrogen saturator gas-liquid interfacial area, cm^2
VOLT:	Net cell voltage, volts
COUT:	Oxygen concentration at electrode exit, 10^{-7} g moles/cc
CHUT:	Hydrogen concentration at electrode exit, 10^{-7} g moles/ cc
TOTP:	Total power consumed, watts
WEOP:	Wt. oxygen electrode, pounds
WEHP:	Wt. hydrogen electrode, pounds
WRADP:	Wt. radiator, pounds
WFP:	Wt. reactants, pounds

WTANKP: Wt. storage tanks, pounds

WSATOP: Wt. oxygen saturator, pounds

WSATHP: Wt. hydrogen saturator, pounds

DENS: Average density of saturator, grams/cm^3

DELPO: Pressure drop oxygen electrode, dynes/cm^2

DELPH: Pressure drop hydrogen electrode, dynes/cm^2

POEL: Oxygen electrode pumping power, gram-wt/cm-sec

PHEL: Hydrogen electrode pumping power, gram-wt/cm-sec

POSAT: Pumping power oxygen saturator per unit electrode area, ergs/sec-cm^2

PHSAT: Pumping power hydrogen saturator per unit electrode area, ergs/sec-cm^2

XLO: Optimized oxygen electrode thickness, cm

XLH: Optimized hydrogen electrode thickness, cm

PROPERTY DATA

T:	System temperature, °K	291	322	373
RES:	Electrolyte resistivity, ohms-cm	1.99	1.26	0.72
DIFH:	Hydrogen diffusivity, (10^{-5} cm^2/sec)	4.36	8.72	17.0
DIFO:	Oxygen diffusivity, (10^{-5} cm^2/sec)	1.79	3.78	7.40
VISC:	Electrolyte viscosity, gram wt/sec-cm	0.0164	0.00825	0.00426
CHQ:	Hydrogen concentration, (10^{-7} g mole/cm^3) (P is saturator pressure, atmospheres)	2.23P	1.88P	1.80P
COQ:	Oxygen concentration	3.13P	2.10P	1.80P

		Pt	Ag
A:	Tafel equation constant (oxygen electrode)	+ 0.096	0.690
B:	Tafel equation constant (oxygen electrode)	+ 0.042	0.130

```
      SUBROUTINE PERF
      COMMON X11,X22,X33,X44,X55,X66,X77,X88,X99,X1010,B1,B2,B3,B4,
     1 B5,B6,B7,B8,B9,B10,C1,C2,C3,C4,C5,C6,C7,C8,C9,C10,D1,D2,D3,D4,
     2 D5,D6,D7,D8,D9,D10,TOCOST,
     3E1,E2,E3,E4,E5,E6,E7,E8,E9,E10,F1,F2,F3,F4,F5,F6,F7,F8,F9,F10
C     UNITS OF ALL INPUTS ARE IN THE CGS SYSTEM
      CFACE=X11
      CLOC=X22
      DO2=X33
      VH2=X44
      DH2=X55
      TIME=X66
      DENS=1.2
      THIC=0.1
      XLSATH=5.0
      XLSATO=5.0
      TSAT=0.0125
      PERM=0.105
C     FIXED INPUTS ARE LISTED IN THE (E) PARAMETERS
      E1=DENS
      E2=THIC
      E3=XLSATH
      E4=XLSATO
      E5=TSAT
34    E6=PERM
      T=D1
      RES=D2
      DIFH=D3
      DIFO=D4
      VISC=D5
      CHQ=D6
      COQ=D7
C     TAFEL EQUATION CONSTANTS ARE CALCULATED FOR LOGARITHMS TO BASE TEN
      A=D8
      B=D9
      CHEQ=CHQ/(10.0**7)
      COEQ=COQ/(10.0**7)
      DIFFH=DIFH/(10.0**5)
      DIFFO=DIFO/(10.0**5)
C     CALCULATION FOR OXYGEN ELECTRODE
    1 C=(9.*RES*CFACE/3.1417)**2-8.*RES*B*CLOC/2.3/DO2
      IF(C) 10,5,5
    5 DELC=0.05
      CFACE=CFACE-DELC
      GO TO 1
   10 XLO =B*2.0*ATANF(9.*RES*CFACE/3.1417/(-C)**0.5)/2.3/(-C)**0.5
      IF(XLO -0.01) 12,12,15
   12 XLO2=0.01
   15 XLO2=XLO
C     CALCULATION FOR HYDROGEN ELECTRODE
C     MASS TRANSFER COEFFICIENT AT CONSTANT WALL CONCENTRATION
   35 XK=3.66*DIFFH/DH2
      CHIN=0.9*CHEQ
      DELVH2=0.1
      Z=9.0*CFACE/(3.1417*VH2*2.0*96540.0*CHIN)
      IF(1.0-Z) 20,20,30
```

```
   20  VH2=VH2+DELVH2
       GO TO 35
   30  XLH =-(VH2*DH2/4.0/XK)*LOGF(1.0-Z)
       IF(XLH -0.01) 40,40,45
   40  XLH2=0.01
   45  XLH2=XLH
C      CALCULATION OF NET CELL VOLTAGE
       V=-A-B/2.3*LOGF(CLOC)
       U=VH2*DH2/4.0/XK
       VOLT=0.92+V-2.0*96540.0*RES*VH2*CHIN*(U-(U-XLH)/EXPF(XLH/U))
      1 -CFACE*RES*2.0*THIC
C      PUMPING POWER REQUIRED PER UNIT AFACE IN GRAM WEIGHTS/CM/SEC
C      POWER FOR OXYGEN ELECTRODE
       COIN=0.9*COEQ
       COOUT=0.2*COIN
       COUT=COOUT*10.0**7
       POEL=(CFACE/(DO2*4.0*96450.0*(COIN-COOUT)))**2
      1 *32.0*VISC*XLO2/981.0*2.25
C      POWER FOR HYDROGEN ELECTRODE
       CHOUT=CHIN-9.0*CFACE/(3.1417*VH2*2.0*96540.0)
       CHUT=CHOUT*10.0**7
       PHEL=(CFACE/(DH2*2.0*96540.0*(CHIN-CHOUT)))**2
      1 *32.0*VISC*XLH2/981.0*2.25
C      PRESSURE DROP THROUGH OXYGEN SATURATOR IN GRAM WT/CM2
       Y=1.0/PERM
       DELPO=Y*DIFFO*8.0*(XLSATO/TSAT)**2/LOGF((COEQ-COOUT)/(COEQ-COIN))
C      PRESSURE DROP THROUGH  HYDROGEN SATURATOR IN GRAM WT/CM2
       DELPH=Y*DIFFH*8.0*(XLSATH/TSAT)**2/LOGF((CHEQ-CHOUT)/(CHEQ-CHIN))
C      POWER REQUIRED FOR OXYGEN SATURATOR PER UNIT AFACE
       POSAT=DELPO*CFACE/(4.0*96540.0*(COIN-COOUT))
C      POWER REQUIRED FOR HYDROGEN SATURATOR PER UNIT AFACE
       PHSAT=DELPH*CFACE/(2.0*96540.0*(CHIN-CHOUT))
C      TOTAL POWER REQUIRED PER UNIT AFACE IN WATTS
       TOPOW =(POEL+PHEL+POSAT+PHSAT)*0.0000981
       AFACE=1000.0/(VOLT*CFACE-TOPOW)
C      TOTAL SYSTEM POWER REQUIRED FOR PUMPING IN WATTS
       TOTP=TOPOW*AFACE
C      SATURATOR AREAS REQUIRED IN CM2
       ASATO=AFACE*CFACE*    TSAT/(4.0*96540.0*4.0*DIFFO*(COIN-COOUT))*
      1 LOGF((COEQ-COOUT)/(COEQ-COIN))
       ASATH=AFACE*CFACE*    TSAT/(2.0*96540.0*4.0*DIFFH*(CHIN-CHOUT))*
      1 LOGF((CHEQ-CHOUT)/(CHEQ-CHIN))
C      PROCESS OUTPUTS ARE LISTED IN THE (B) PARAMETERS
       B1=XLO2
       B2=XLH2
       B3=AFACE
       B4=ASATO
       B5=ASATH
       B6=VOLT
       B7=COUT
       B8=CHUT
       B9=TOTP
       B10=V
       E10=CFACE
C      PRESSURE DROPS AND POWER CONSUMPTION PER UNIT AFACE ARE
       F1=DELPO
```

```
F2=DELPH
F3=POEL
F4=PHEL
F5=VH2
F6=POSAT
F7=PHSAT
F9=XLO
F10=XLH
RETURN
END(1,0,0,0,0,0,0,0,0,0,0,0,0,0,0)
```

```
      SUBROUTINE COST
      COMMON X11,X22,X33,X44,X55,X66,X77,X88,X99,X1010,B1,B2,B3,B4,
     1 B5,B6,B7,B8,B9,B10,C1,C2,C3,C4,C5,C6,C7,C8,C9,C10,D1,D2,D3,D4,
     2 D5,D6,D7,D8,D9,D10,TOCOST,
     3E1,E2,E3,E4,E5,E6,E7,E8,E9,E10,F1,F2,F3,F4,F5,F6,F7,F8,F9,F10
C     WEIGHTS ENDING IN (G) DENOTE GRAMS.
C     WEIGHTS ENDING IN (P) DENOTE POUNDS
C     WEIGHT OF THE OXYGEN ELECTRODE
      WEOG=B3*(B1*6.92+E2*1.2)
      WEOP=WEOG/454.0
C     WEIGHT OF THE HYDROGEN ELECTRODE
      WEHG=B3*(B2*6.92+E2*1.2)
      WEHP=WEHG/454.0
C     RADIATOR AREA CALCULATION
      ARAD=((B3*E10*1.25)-1000.0)*10.**7/(0.0000571*D1**4)
C     SPECIFIC MASS OF RADIATOR IS 1 LB/FT2 AREA
      WRADP=ARAD/929.0
C     WEIGHT OF FUEL REQUIRED
      WFP=B3*E10*3600.0*18.0*X66/(2.0*96540.0*454.0)
C     TANK WEIGHT TAKEN TO BE ONE-HALF FUEL WEIGHT
      WTANKP=0.5*WFP
C     WEIGHT OF SATURATORS -OXYGEN
      WSATOG=B4*E5*3.25/2.0
      WSATOP=WSATOG/454.0
C                          - HYDROGEN
      WSATHG=B5*E5*3.25/2.0
      WSATHP=WSATHG/454.0
C     TOTAL FUEL CELL WEIGHT IN POUNDS/KW FOR GIVEN MISSION LENGTH=TOCOS
      TOCOST=WEOP+WEHP+WRADP+WFP+WTANKP+WSATOP+WSATHP
      C1=WEOP
      C2=WEHP
      C3=WRADP
      C4=WFP
      C5=WTANKP
      C6=WSATOP
      C7=WSATHP
      RETURN
      END(1,0,0,0,0,0,0,0,0,0,0,0,0,0,0)
```

Appendix C

COMPUTER PRINTOUT FOR A TYPICAL CASE

THE VALUE OF THE X PARAMETERS ARE SHOWN BELOW , Pt CATALYZED O_2 ELECTRODE , 50 ATM. SATURATORS . 18°C

0.18000	0.00575	0.00050	0.29000	0.00050
24.00000	0.	0.	0.	0.

THE VALUE OF THE B PARAMETERS ARE SHOWN BELOW

0.01438	0.00028	6686.74573	101611.67285	107981.65332
0.84642	28.17000	8.25947	18.75958	-0.00180

THE VALUE OF THE C PARAMETERS ARE SHOWN BELOW

3.23299	1.79633	13.26333	21.35406	10.67703
4.54623	4.83123	0.	0.	0.

THE VALUE OF THE D PARAMETERS ARE SHOWN BELOW

291.00000	1.99000	4.36000	1.79000	0.01640
111.50000	156.50000	0.09600	0.04200	0.

THE VALUE OF THE E PARAMETERS ARE SHOWN BELOW

1.20000	0.10000	5.00000	5.00000	0.01250
0.10500	0.	0.	0.	99.90000

THE VALUE OF THE F PARAMETERS ARE SHOWN BELOW

103.70514	238.81178	0.11870	0.01400	0.
4.29001	24.17553	0.	0.01438	0.00028

402 WH/lb

OPTIMIZED FUEL CELL WEIGHT IN LBS/KW 59.70119

THE VALUE OF THE X PARAMETERS ARE SHOWN BELOW

0.15000	0.00500	0.00050	0.29000	0.00050
96.00000	0.	0.	0.	0.

THE VALUE OF THE B PARAMETERS ARE SHOWN BELOW

0.01301	0.00016	7922.58643	100326.24023	118686.54785
0.86091	28.17000	23.60789	23.09686	0.00075

THE VALUE OF THE C PARAMETERS ARE SHOWN BELOW

3.66481	2.11392	12.76298	84.33568	42.16784
4.48872	5.31018	0.	0.	0.

THE VALUE OF THE D PARAMETERS ARE SHOWN BELOW

291.00000	1.99000	4.36000	1.79000	0.01640
111.50000	156.50000	0.09600	0.04200	0.

THE VALUE OF THE E PARAMETERS ARE SHOWN BELOW

1.20000	0.10000	5.00000	5.00000	0.01250
0.10500	0.	0.	0.	99.90000

THE VALUE OF THE F PARAMETERS ARE SHOWN BELOW

103.70514	257.42837	0.07456	0.00811	0.
3.57501	26.06013	0.	0.01301	0.00016

OPTIMIZED FUEL CELL WEIGHT IN LBS/KW 154.84411

620 WH/Lb

THE VALUE OF THE X PARAMETERS ARE SHOWN BELOW

0.13000	0.00500	0.00050	0.19500	0.00050
240.00000	0.	0.	0.	0.

THE VALUE OF THE B PARAMETERS ARE SHOWN BELOW

0.01069	0.00032	9000.54272	98779.84473	100542.47852
0.86895	28.17000	1.43794	16.73489	0.00075

THE VALUE OF THE C PARAMETERS ARE SHOWN BELOW

3.84618	2.42348	12.16104	207.58939	103.79489
4.41953	4.49839	0.	0.	0.

THE VALUE OF THE D PARAMETERS ARE SHOWN BELOW

291.00000	1.99000	4.36000	1.79000	0.01640
111.50000	156.50000	0.09600	0.04200	0.

THE VALUE OF THE E PARAMETERS ARE SHOWN BELOW

1.20000	0.10000	5.00000	5.00000	0.01250
0.10500	0.	0.	0.	99.90000

THE VALUE OF THE F PARAMETERS ARE SHOWN BELOW

103.70514	232.13820	0.04605	0.00723	0.
3.09834	15.80169	0.	0.01069	0.00032

OPTIMIZED FUEL CELL WEIGHT IN LBS/KW 338.73269

708 WH/Lb